Journal of Hydrology: Regional Studies 60 (2025) 102530

Contents lists available at ScienceDirect

Journal of Hydrology: Regional Studies

journal homepage: www.elsevier.com/locate/ejrh

Innovative use of reanalysis data in Slovenia: Enhancing precipitation time series with a multiplicative cascade model

Hannes Müller-Thomy [a,1,2,*], Jana Kellner [a,b,3], Patrick Nistahl [c,4], Nejc Bezak [d,5], Katarina Zabret [d,6], Kai Schröter [a,7]

[a] *Leichtweiß Institute for Hydraulic Engineering and Water Resources, Division of Hydrology and River Basin Management, Technische Universität Braunschweig, Brunswick, Germany*
[b] *Wasserverband Peine, Peine, Germany*
[c] *Harzwasserwerke GmbH, Hildesheim, Germany*
[d] *Faculty of Civil and Geodetic Engineering, University of Ljubljana, Ljubljana, Slovenia*

ARTICLE INFO

Keywords:
ERA5-Land
COSMO-REA6
Reanalysis products
Precipitation
Rainfall generator
Cascade model
Disaggregation

ABSTRACT

Study region: Slovenia
Study focus: Precipitation reanalysis products (PRP) with hourly resolution as ERA5-Land and COSMO-REA6 are a promising solution for hydrologic applications in data scarce regions as Slovenia. Both data sets are validated against observed hourly time series from 5 rain gauges and areal precipitation in 20 catchments in Slovenia regarding continuous and event-based precipitation characteristics as well as extreme values. Both, station and catchment precipitation are not well-represented by PRP, with a worse representation by ERA5-Land than COSMO-REA6. The aim of this study is to explore how if the PRP time series can, instead of being directly appliedtime series, from precipitation reanalysis products (PRP) can be used for the generation of high-resolution precipitation time series in unobserved catchments. A new approach is proposed to estimate parameters of a micro-canonical cascade model from ERA5-Land and COSMO-REA6 time series to generate hourly time series from daily observations.
New hydrologic insights for the region: The proposed parameter estimation approach leads to a general better representation of precipitation characteristics. For some stations the disaggregation based on COSMO-REA6 parameters even outperforms disaggregation results with parameters estimated from observed time series at these stations. Significant spatial patterns of PRP errors are identified which can help improving future PRP. The parameterization approach is not limited to the study region and can be used for precipitation generation in unobserved catchments, particularly in catchments with complex terrain which are usually not well represented by PRP.
Plain language summary: For many hydrological applications precipitation data with hourly resolution are required. Unfortunately, this kind of data exists often only for a few stations or only

* Corresponding author.
E-mail address: h.mueller-thomy@tu-braunschweig.de (H. Müller-Thomy).
[1] Previously published under the name Hannes Müller
[2] 0000-0001-5214-8945
[3] 0009-0000-0266-1046
[4] 0000-0001-9000-8249
[5] 0000-0003-2264-1901
[6] 0000-0001-7097-3818
[7] 0000-0002-3173-7019

https://doi.org/10.1016/j.ejrh.2025.102530
Received 27 January 2025; Received in revised form 9 May 2025; Accepted 12 June 2025
Available online 21 June 2025

for short periods in the region of interest. Precipitation reanalysis data (PRP), which are produced by simulating the earth's atmosphere over the last decades, are a promising solution. However, the quality of PRP depends on multiple factors and has to be tested for each region before application. In this study widely used ERA5-Land and COSMO-REA6 are tested for five rain gauges and 20 catchments in Slovenia. The validation of PRP with available observations for the study area indicated strong deviations. So instead of using the PRP directly for hydrological applications, a precipitation generator was parameterized with information from the PRP. Its validation shows a better representation of the observations, which suggests their usage for subsequent hydrological applications.

1. Introduction

High-resolution rainfall time series are required for many hydrological applications, e.g. rainfall-runoff modelling (Ding et al., 2016), urban hydrology studies (Müller and Haberlandt, 2018; Derx et al., 2023) and erosion studies (Dunkerley, 2019; Pidoto et al., 2022). Blöschl and Sivapalan (1995) showed that hydrologic processes differ regarding their dynamics, hence different resolutions in space and time are required to illustrate these processes adequately in hydrologic models. For urban hydrologic models temporal resolutions of 5 min and finer are required (Schilling, 1991; Ochoa-Rodriguez et al., 2015). Catchment rainfall-runoff models often use hourly time series for mesoscale catchments (~50–1000 km^2; e.g., Ding et al., Müller-Thomy et al., 2018; Alexopoulos et al., 2023). Also, for a sufficient representation of the areal rainfall high station densities are required (e.g. Krajewski et al., 1991; Ogden and Julien, 1993; Obled et al., 1994; Nicotina et al., 2008).

Observed time series with hourly resolution are often not available with either the required spatial density or the time series length as required for e.g. subsequent flood frequency analysis. There are two possible solutions to solve this data scarcity: i) the usage of precipitation reanalysis products (PRP) or ii) generation of hourly rainfall time series.

PRP are a combination of data assimilation and numerical simulations of the global atmosphere over the last decades (Dee et al., 2011). Due to the assimilated data sources PRP can outperform single observational data sets (e.g., Gebremichael et al., 2017; Gu et al., 2023). Since PRP with finer resolution can represent precipitation better in space and time than with coarser resolution (Gustafsson and Dahlgren, 2012; Wahl et al., 2017), this study focusses on ERA5-Land and COSMO-REA6 as promising solutions from the latest generation of PRP.

ERA5-Land (Munoz-Sabater et al., 2021) provides climate data with horizontal resolution of approximately 9 km and temporal resolution of 1 h. It is a refinement of the ERA5 level 137 (10 m close to the surface) by triangular interpolation for the land component of ERA5 (Δl=31 km, Δt = 1 h, Hersbach et al., 2020), which replaced ERA-Interim (Δl=79 km, Δt = 6 h, Berrisford et al., 2009). ERA5-Land covers the period from 1940 onwards, which exceeds all available high-resolution rainfall data sets. COSMO-REA6 (Δl=6 km, Δt = 1 h, Bollmeyer et al., 2015) resulted from the consortium for small-scale modelling (COSMO) limited-area model (LAM), a numerical weather prediction model from the German Weather Service, and covers the period 1995–2019. Since ERA-Interim was used as a boundary condition for LAM, COSMO-REA6 ended with the introduction of ERA5.

However, there are several potential shortcomings related to the selected PRP. Bandhauer et al. (2022) identified, for selected regions in Europe, a general overestimation of all monthly precipitation amounts and wet-day frequencies for ERA5, with stronger overestimations in the high-mountainous catchments in the summer period. This is confirmed by Dalla Torre et al. (2024), who report an overestimation of annual rainfall amounts by ERA5-Land for South-Tyrol. Sharifi et al. (2019) report weaknesses for daily rainfall amounts of ERA5 at high altitude and in complex terrain as Alpine valleys in Austria. However, precipitation peaks in October and November are underestimated, probably "due to limited resolution of related mesoscale processes" (Bandhauer et al., 2022). The general overestimation of rainfall amounts and wet days, but simultaneous underestimation of high rainfall amounts is confirmed by Bliznak et al. (2022) for ERA5 and ERA5-Land for the Czech Republic.

Dahlgren et al. (2016) validated ERA-Interim on a continental scale for Europe and found that it underestimates the number of intensive rainfall events (≥20 mm/d), but overestimates the number of days with intensities ≤ 0.1 mm/d. Isotta et al. (2015) identified for Central and Southern Europe an underestimation of the mean rainfall intensity by ERA-Interim by a simultaneous overestimation of wet day frequency. Large-scale patterns of rainfall-intense regions are not represented by ERA-Interim (Isotta et al., 2015). Lockhoff et al. (2019) identified for the mean rainfall intensity for Slovenia both, slight underestimations in the north and slight overestimations in the south by COSMO-REA6.

Following conclusions can be made based on this literature review, i) an advantage of high-resolution reanalysis data is the better representation of small-scale variability, and ii) extreme values are better represented by regional reanalysis data than global data sets (Gustafsson und Dahlgren 2012; Kaiser-Weiss et al., 2019; Lockhoff et al., 2019). However, depending on the region, deviations will differ quantitatively (Isotta et al., 2015). Consequently, PRP have to be evaluated for the data scarce region of interest and not for a different region with more data available.

If a PRP validation indicates a limited applicability of the PRP for the intended application in the study region, rainfall generation is a promising alternative. Parameters of stochastic rainfall generators can be estimated from observed time series which are shorter than required for the intended application or from time series at meteorologically similar locations. Among numerous stochastic rainfall generators as pulse models and alternating renewal models, the micro-canonical cascade models (MCM) have the advantage that the starting point for the rainfall generation are observed time series with daily resolution. The daily rainfall amount is conserved exactly throughout the disaggregation process. Daily time series exist from non-recording stations with a high network density and often cover long measuring periods. Starting from daily values, the MCM can generate finer and finer temporal resolutions until a final temporal resolution is achieved (e.g. Olsson, 1998; Güntner et al., 2001). MCM have been used to generate precipitation time series worldwide. For this study, only findings for study areas close to Slovenia as region of interest are discussed below.

For the generation of time series with 10-minute resolution in Switzerland, Molnar and Burlando (2005) compared a MCM with a canonical cascade model, which conserves the daily rainfall amounts not exactly, but on average. The MCM reproduced well the intermittency of the rainfall process and also the annual maxima. However, the cumulative distribution function of rainfall intensities showed a general overestimation of rainfall intensities, and a high fraction of rainfall intensities smaller than the minimum temporal resolution (caused by the accuracy of the measuring instrument) used for parameter estimation. Although Molnar and Burlando (2005) studied only one observed time series, this problem was confirmed by e.g. Müller and Haberlandt (2008) and resolved in Müller-Thomy (2020). Derx et al. (2023) validated a MCM at five Viennese stations in Austria and the identified performance regarding extreme values (observed extreme values are within the range of disaggregation results), continuous (relative error for average intensity: −3 %, probability of dry time steps: −1 %) and event-based characteristics (wet spell amount: 4 %, wet spell duration: 7 %) reasoned the choice of the MCM for the subsequent disaggregation of climate model data. Ebers et al. (2024) introduced temperature-dependency of MCM parameters to increase the physical plausibility of MCM to disaggregate future climate model data.

Besides the station-based disaggregation, MCM have been used for the temporal disaggregation of areal rainfall. Müller-Thomy and Sikorska-Senoner (2019) validated MCM for nine Swiss catchments with daily areal rainfall values derived from the interpolation of observed daily time series. They found that the relative error was very similar between station-based and areal-based disaggregation results ($\Delta t = 1$ h) for continuous and event-based characteristics. Extreme values were also well represented by the variant implemented from Müller and Haberlandt (2015). For Switzerland, Maloku et al. (2024) disaggregated daily areal rainfall time series, which were generated before by GWEX (following Richardson (1981), Wilks (1998) and Evin et al. (2018)). Maloku et al. (2024) showed that the performance of the applied MCM depends on seasons and studied area size. In general, the performance improves with increasing catchment size for the studied continuous and event-based precipitation characteristics, as well as for the extreme values.

For a robust estimation of MCM parameters, a minimum time series length is required, since short time series may not be representative for the overall rainfall behavior. Müller (2016) identified a minimum length of seven years as compromise between parameter variation and number of appropriate stations for Lower Saxony, Germany.

However, the authors are not aware of any references comparing the effects of spatial and temporal availability, e.g. if it is recommended to use a closer, but shorter time series rather than a station far off, but providing a longer time series. Due to regional differences of rainfall behavior the authors expect no general answer to this hypothetic question. Nevertheless, since the intrinsic motivation for rainfall generation is the lack of suitable rainfall information at certain locations, the question remains: How can MCM parameters be estimated for locations without any observations? Since reanalysis products are available for decades of rainfall data for each location in their respective domain, they seem to be a promising source for MCM parameter estimation.

In this study the PRP ERA5-Land and REA6 will first be validated for Slovenia and subsequently tested regarding their suitability for the estimation of MCM parameters. To the best of authors knowledge this will be the first time that reanalysis data will be used for estimation of MCM parameters. However, the incorporation of PRP was studied for other rainfall generators before for AWE-GEN-2d (Peleg et al., 2020) and method-of-fragments (Acharya et al., 2022) as described in the following. Peleg et al. (2020) applied a bias-corrected version of CMORPH reanalysis data (Xie et al., 2017) to calibrate the rainfall module of the weather generator AWE-GEN-2d (Peleg et al., 2017, 2019) for the Zambezi river basin, Africa. Although the validation of the CMORPH dataset showed underestimation of the annual rainfall amounts, the simulated annual rainfall amounts were within the range of the natural climate variability for the study area. Acharya et al. (2022) apply a relatively simple, non-parametric disaggregation method known as method-of-fragment (Breinl and Di Baldassarre, 2019) for Australia. Acharya et al. (2022) use relative hourly rainfall patterns from BARRA-R reanalysis data (Su et al., 2019) to disaggregate observed daily rainfall amounts from AWAP (National Australian dataset, Jones et al., 2009). Acharya et al. (2022) show by a gauge-based validation that although the direct usage of BARRA-R cannot be recommended, using BARRA-R for parameter estimation improves the disaggregated rainfall time series regarding mean rainfall intensity, skewness coefficient of rainfall intensities and frequency of wet time steps. However, for some criteria as the variation coefficient of rainfall intensities and transition probabilities the results are worsening. Therefore, the main objective of this study is to test if MCM parameters can be estimated for locations without any observations from PRP to generate high-resolution rainfall time series.

The manuscript is structured in five sections. The introduction in 1 is followed by a description of the data in 2. In 3 the applied micro-canonical cascade model and the validation procedure are explained. Validation results for rain gauges and catchments are shown and discussed in Sections 4.1 and 4.2, respectively, and identified deviations are analyzed regarding their dependency on catchment attributes in 4.3. Conclusions are provided in 5.

2. Data

The Sections 2.1, 2.2 and 2.3 contain detailed information about respectively: the observed data, the PRP and the catchment data applied in this study.

2.1. Observation

Three observation data sets were applied in this study (Table 1): rain gauge data, radar data and the ARSO data set. The rain gauge data set refers to five time series with hourly resolution. The ARSO data set (from here referred to as ARSO) is a regionalized precipitation product from the Slovenian Environment Agency, which is available for the whole country with a spatial and temporal resolution of 1 km raster width and 1 day, respectively. The radar data set was also available for whole Slovenia, with a spatial and temporal resolution of 1 km raster width and 1 h, respectively.

Since for the validation of the PRP a spatial reference data set with hourly resolution was required, the ARSO and radar data were merged. Therefore, for each day and raster cell the relative diurnal cycle from the radar data was used to distribute the daily rainfall amounts from ARSO for this raster cell over the 24 h of the respective day. The resulting data set includes the daily rainfall amounts from ARSO as reference data set and the diurnal temporal distribution from the radar data. This merged data set is referred to as ARSO-h and was used as spatial reference for all PRP comparisons.

Areal rainfall time series for the catchment-based comparisons were derived as areal-weighted mean of all raster cells within the catchment boundary.

2.2. Reanalysis data

Two PRP were validated for Slovenia in this study: ERA5-Land and COSMO-REA6. ERA5-Land is available globally for 1950–2024 and based on ERA5 (Hersbach et al., 2020), which is provided by the Copernicus Climate Change Service at the European Centre for Medium-Range Weather Forecasts (ECMWF). For ERA5-Land the spatial resolution is increased for the land components from 31 km raster width (ERA5) to 9 km raster width by maintaining the hourly resolution (Muñoz-Sabater et al., 2021).

COSMO-REA6 (Bollmeyer et al., 2015) has an even finer spatial resolution with 6 km raster width for whole Europe. COSMO-REA6 was provided by the Consortium for Small-Scale Modelling (COSMO), a numerical weather prediction of the German Weather Service (DWD). The boundary condition for COSMO were ERA5-Interim data. Since ERA5-Interim got replaced by ERA5, the COSMO-REA6 data is limited to the period 1995–2019 with currently no option for extension.

Areal rainfall time series of the PRP were derived identically to the observed data.

2.3. Catchments

In general, the Slovenian climate is strongly related to its orography (e.g., Dolšak et al., 2016) and offers the possibility to study the approach across different climate classes. Following the classification scheme after Köppen (Peel et al., 2007) a temperate climate without dry season but warm summers (Cfb) can be found in the lowlands of southern Slovenia, which are connected to the Adriatic Sea. The increasing altitude towards the north leads to cold climates without dry season but warm summers (Dfb) and for higher regions with cold summers (Dfc). For the alpine region with elevations up to 2864 m a.s.l. (Mount Triglav) polar (Tundra) climate (ET) is identified.

For an areal-based validation of the PRP the 20 catchments in Fig. 1 are used. Topographic catchment information is provided in Table 1. Hydrologic characteristics of the catchments are described by Alexopoulos et al. (2023). The areal rainfall time series of ARSO-h, ERA5-Land and REA6 were derived for each time step by weighting the rainfall amounts of all raster cells within a catchment based on their areal contribution.

3. Methods

3.1. Cascade model

For the generation of hourly precipitation time series from daily time steps the micro-canonical cascade (MCM) model after Müller and Haberlandt (2015) is applied, which exactly conserves the rainfall amount within one day. Based on the principle of self-similarity, the rainfall distribution on a fine time scale can be concluded from the rainfall distribution on a coarser scale. Starting with daily values, in each disaggregation step b finer time steps with same duration are generated, with b as branching number. For the first disaggregation step $b = 3$ is applied ($\Delta t = 24\ h \rightarrow 8\ h$), for all subsequent disaggregation steps $b = 2$ is chosen ($\Delta t = 8\ h \rightarrow 4\ h \rightarrow 2\ h \rightarrow 1\ h$). Details on the applied cascade model and its parameters are provided in the supplementary material A.

3.2. Validation

The suitability of reanalysis data for the estimation of the cascade model parameters for disaggregation is validated for station-based and catchment-based precipitation disaggregation (Fig. 2). For both, observed hourly precipitation time series are aggregated to daily values. So for the station-based disaggregation the time series length of the disaggregation object is identical with the time series length reported in Table 1 (‘OBS’), for the catchment-based disaggregation ARSO is limited to 2006–2010 due to the data availability of ARSO-h limited to this period.

The daily time series are disaggregated afterwards with parameter sets estimated from observations or PRP. For the parameter estimation, the whole time series of observations and PRP were used.

The parameters estimated from observations and PRP are analyzed and compared, followed by a validation of the disaggregated time series regarding continuous (average intensity, fraction of dry intervals) and event-based precipitation characteristics (wet and dry spell duration, wet spell amount) as well as extreme values. Precipitation events are defined as wet time step(s) surrounded by at least one dry time step before and after the event, whereby dry refers to a precipitation amount of 0 mm.

Extreme values were selected by peak-over-threshold method. The threshold was chosen in such a way that the resulting population

Table 1
Metadata of rain gauge and catchments as time series length, physiographic attributes (altitude, catchment area) and precipitation characteristics.

Data set	Name	Station / Closest station	Catchment ID	Time series length	Altitude [m a.s.l.]	Area [km^2]	Missing values [%]	Annual Precipitation [mm]	Fraction of wet time steps [%]	Wet spell duration [Δt]	Wet spell amount [mm]	Dry spell duration Δt	Average intensity [mm/Δt]
OBS [Δt = 1 h]	Log pod Mangartom	A	-	1999 - 2017	648	-	44.9	2405	7.9	3.8	6.6	22.4	1.7
	Postojna	B	-	1970 - 2017	533	-	53.7	1535	5.8	3.1	4.2	21.3	1.3
	Smartno pri Slov. Gr.	C	-	1990 - 2017	445	-	58.3	1190	5.4	3.1	3.6	20.4	1.2
	Murska Sobota	D	-	1970 - 2017	188	-	56.2	805	4.2	2.8	3.0	25.8	1.1
	Bohinsjska Bistrica	E	-	2002 - 2017	507	-	71.4	2141	4.1	3.3	5.0	19.3	1.5
ARSO [Δt = 1d]	Mislinja-Otiški vrh	C	1	1981 - 2010	773.4	231.9	-	1299.2	56.5	3.8	24.1	2.9	6.3
	Dravinja-Zreče	C	2	1981 - 2010	884.1	42.6	-	1283.6	54.2	3.5	22.6	2.9	6.5
	Pesnica-Zamušani	D	3	1981 - 2010	291.2	480.8	-	942.9	54.9	3.6	16.7	2.9	4.7
	Radovna-Podhom	E	4	1981 - 2010	1192.9	167.1	-	2009.5	57.1	4.0	38.9	3.0	9.6
	Kokra-Kokra	E	5	1981 - 2010	1251	113.1	-	1770.1	56.7	3.9	33.7	3.0	8.5
	Poljanska Sora-Zminec	E	6	1981 - 2010	683.2	306.5	-	1780.0	57.6	4.2	35.4	3.1	8.5
	Selška Sora-Železniki	E	7	1981 - 2010	944.8	104.1	-	1908.5	56.3	4.0	37.3	3.1	9.3
	Mirna-Jelovec	C	8	1981 - 2010	417.3	271.2	-	1166.3	57.5	4.0	22.4	3.0	5.6
	Kolpa-Petrina	B	9	1981 - 2010	827.1	467.3	-	1877.4	59.4	4.4	37.9	3.0	8.7
	Lahinja-Gradac	B	10	1981 - 2010	316.1	219.1	-	1288.7	55.9	3.9	24.3	3.0	6.3
	Cerkniščica-Cerknica	B	11	1981 - 2010	723.3	49.4	-	1538.1	55.9	3.9	29.4	3.1	7.5
	Savinja-Nazarje	C	12	1981 - 2010	948.6	457.1	-	1625.8	58.2	4.1	31.7	3.0	7.6
	Bolska-Dvas	C	13	1981 - 2010	576.9	170.6	-	1376.5	57.2	4.0	26.3	3.0	6.6
	Voglanja-Crnolica	C	14	1981 - 2010	388.5	54.7	-	1114.5	53.4	3.5	19.8	3.0	5.7
	Hudinja-SVas	C	15	1981 - 2010	609.8	155.9	-	1196.3	55.9	3.8	22.1	3.0	5.9
	Soča-Kobarid	A	16	1981 - 2010	1215.3	437.1	-	2730.0	58.3	4.2	54.4	3.0	12.8
	Idrijca-Hotešk	E	17	1981 - 2010	688.9	443.5	-	2057.7	58.0	4.3	41.5	3.1	9.7

(*continued on next page*)

Table 1 (*continued*)

Data set	Name	Station / Closest station	Catchment ID	Time series length	Altitude [m a.s.l.]	Area [km^2]	Missing values [%]	Annual Precipitation [mm]	Fraction of wet time steps [%]	Wet spell duration [Δt]	Wet spell amount [mm]	Dry spell duration Δt	Average intensity [mm/Δt]
	Bača-Bača pri Modreju	E	18	1981 - 2010	836.2	143.1	-	2357.0	56.8	4.1	46.4	3.1	11.4
	Reka-CMlin	B	19	1981 - 2010	588.3	332.1	-	1524.6	57.4	4.3	30.9	3.2	7.3
	Rižana-Kubed	B	20	1981 - 2010	596.1	204.7	-	1461.0	55.7	4.0	29.0	3.2	7.2
Radar [Δt = 1 h]	Mislinja-Otiški vrh	C	1	2006 - 2010	773.4	231.9	10.1	1146.8	19.1	4.2	2.8	15.6	0.7
	Dravinja-Zreče	C	2	2006 - 2010	884.1	42.6	8.2	1070.5	12.4	3.6	3.3	22.0	0.9
	Pesnica-Zamušani	D	3	2006 - 2010	291.2	480.8	8.9	808.0	16.2	4.9	2.6	22.0	0.5
	Radovna-Podhom	E	4	2006 - 2010	1192.9	167.1	10.0	1861.6	22.0	4.5	4.1	13.7	0.9
	Kokra-Kokra	E	5	2006 - 2010	1251	113.1	8.7	1400.9	11.4	2.8	3.8	18.8	1.4
	Poljanska Sora-Zminec	E	6	2006 - 2010	683.2	306.5	10.2	1602.5	20.3	4.8	4.1	16.2	0.9
	Selška Sora-Železniki	E	7	2006 - 2010	944.8	104.1	8.9	1537.7	13.2	4.5	5.8	25.8	1.3
	Mirna-Jelovec	C	8	2006 - 2010	417.3	271.2	9.6	943.5	16.5	5.2	3.2	22.4	0.6
	Kolpa-Petrina	B	9	2006 - 2010	827.1	467.3	11.6	1740.5	27.5	5.7	3.9	12.7	0.7
	Lahinja-Gradac	B	10	2006 - 2010	316.1	219.1	9.3	1066.9	17.9	4.7	3.1	18.8	0.7
	Cerkniščica-Cerknica	B	11	2006 - 2010	723.3	49.4	8.7	1313.6	16.1	4.3	3.9	19.6	0.9
	Savinja-Nazarje	C	12	2006 - 2010	948.6	457.1	10.6	1477.2	24.0	4.7	3.1	12.8	0.7
	Bolska-Dvas	C	13	2006 - 2010	576.9	170.6	9.3	1172.1	16.8	4.3	3.2	18.5	0.8
	Voglanja-Crnolica	C	14	2006 - 2010	388.5	54.7	7.8	881.6	11.3	4.3	3.6	29.0	0.8
	Hudinja-SVas	C	15	2006 - 2010	609.8	155.9	9.0	1017.2	17.2	4.2	2.7	17.5	0.6
	Soča-Kobarid	A	16	2006 - 2010	1215.3	437.1	10.9	2413.8	24.0	4.6	5.0	12.5	1.1
	Idrijca-Hotešk	E	17	2006 - 2010	688.9	443.5	11.5	1916.0	27.5	5.4	4.0	12.1	0.7
	Bača-Bača pri Modreju	E	18	2006 - 2010	836.2	143.1	9.3	1871.9	14.0	5.0	7.3	26.1	1.5
	Reka-CMlin	B	19	2006 - 2010	588.3	332.1	9.5	1365.5	18.0	6.4	5.2	24.5	0.8
	Rižana-Kubed	B	20	2006 - 2010	596.1	204.7	8.8	1313.8	15.2	5.3	5.0	25.4	0.9

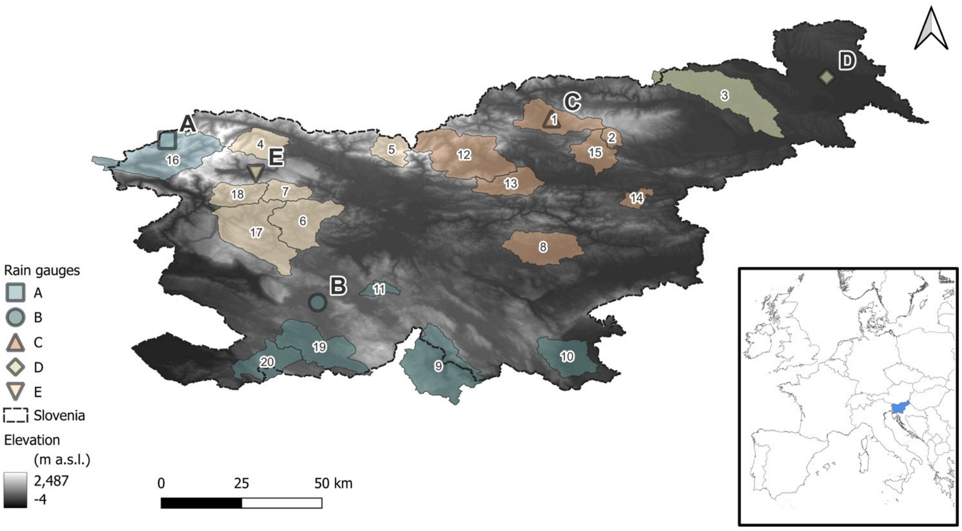

Fig. 1. Rain gauges and catchments used for PRP validation. The colors of each catchment identify the closest rain gauge. The map in the lower left corner shows the location of Slovenia in Europe (highlighted in blue). (sources: European countries: Sevdari and Marmullaku 2023; digital elevation model: Jarvis et al., 2008).

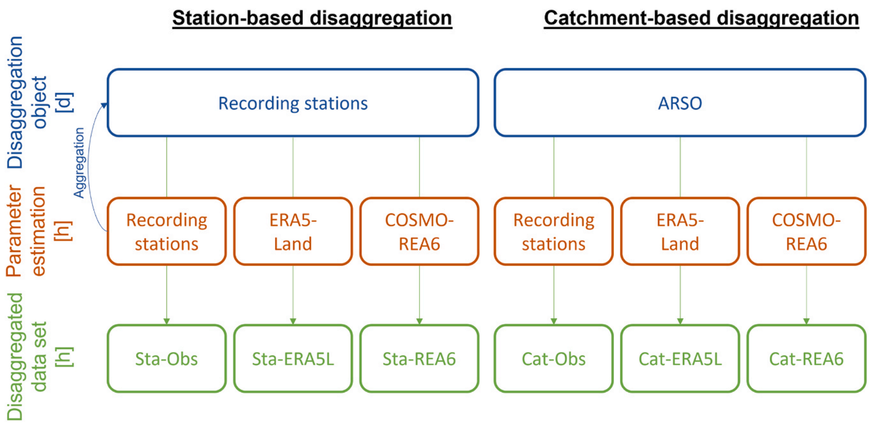

Fig. 2. Workflow overview and applied data sets for station-based and catchment-based validation of precipitation disaggregation with the identification of the time step used (i.e., daily-d and hourly-h).

is three times the length of the respective time series. The independence of the extreme events is ensured by a minimum of 4 dry hours between the events for extreme event durations $D \leq 4$ h, and for $D > 4$ h by a minimum dry spell duration as long as the studied extreme event duration (DWA-A 531, 2012). Return periods T_n are estimated by plotting positions in dependence of length of time series M, population size L and index k (running from k = 1 as largest to k = L as smallest values):

$$T_n = \frac{L + 0.2}{k - 0.4} \bullet \frac{M}{L} \tag{1}$$

The errors resulting from the disaggregation in comparison to the observations (OBS) are quantified for precipitation characteristics (PC) over all stations n and all realizations m of the disaggregation (DIS) by the mean absolute error MAE (Eq. 2) and the relative error PBIAS (Eq. 3):

$$MAE = \frac{1}{n \bullet m} \bullet \sum\nolimits_{j=1}^{n} \sum\nolimits_{i=1}^{m} PC_{DIS,i,j} - PC_{OBS,j} \tag{2}$$

$$PBIAS = \frac{1}{n \bullet m} \bullet \sum\nolimits_{j=1}^{n} \sum\nolimits_{i=1}^{m} \frac{PC_{D,i,j} - PC_{O,j}}{PC_{O,j}} \tag{3}$$

4. Results and discussion

The PRP are validated for the 5 recording stations (Sect. 4.1) and for the 20 catchments (Sect. 4.2) if i) applied directly and ii) if used for cascade model parameter estimation and subsequently precipitation disaggregation.

4.1. Station-based PRP validation

The validation results of the PRP time series are shown in Fig. 3 and Table 2 for continuous and event-based precipitation characteristics. Both, ERA5-Land and COSMO-REA6, lead to a strong overestimation for wet spell duration, and strong underestimation of dry spell duration, wet spell amount, fraction of dry intervals and average intensity. This could be expected due to the larger spatial extent of the PRP (ERA5-Land: ~81 km^2, REA6: ~36 km^2) in comparison to a rain gauge (e.g., Reinhold rain gauge: 200 cm^2). The larger the spatial extent, the higher is the probability to include a rainfall event, which causes longer wet spell events with smaller intensities and shorter dry spells in between. Thus, for ERA5-Land the deviations are higher than for REA6 due to the coarser spatial resolution of ERA5-Land.

The precipitation characteristics of the disaggregated time series depend on the cascade model parameters and hence on the data set used for their estimation. Details on all estimated parameters are provided in the supplementary material B. In general, a systematic underestimation of probabilities leading to dry time step is identified when PRP are used for the parameter estimation, while probabilities leading to only wet time steps are systematically overestimated. Although this systematic is identical for ERA5-Land and COSMO-REA6, the parameters estimated from COSMO-REA6 are closer to parameters estimated from observations. The results of the disaggregated time series are also included in Fig. 3 and Table 2.

The disaggregated time series using parameters estimated from observed time series are used for the validation of the cascade model regarding its applicability in Slovenia. The deviations of wet spell amount, dry spell duration and fraction of dry intervals with |PBIAS| < 10 % can be considered as small and proof the applicability of the cascade model. PBIAS for wet spell amount (-18 %) and average intensity (13 %) are higher. However, both precipitation characteristics are interdependent and deviations of this magnitude are typical for the applied cascade model (see Müller and Haberlandt, 2015, for Germany; and Müller-Thomy and Sikorska-Senoner, 2019, for Switzerland). An extension of the set of position classes for parameter estimation (Müller-Thomy, 2020) could be a possible solution as shown by Pidoto et al. (2022). The cascade model suggested by Güntner et al. (2001) using b= 2 for all disaggregation steps was tested as an alternative in a pre-study by Kellner (2022), but the results were outperformed by the cascade model variant applied in

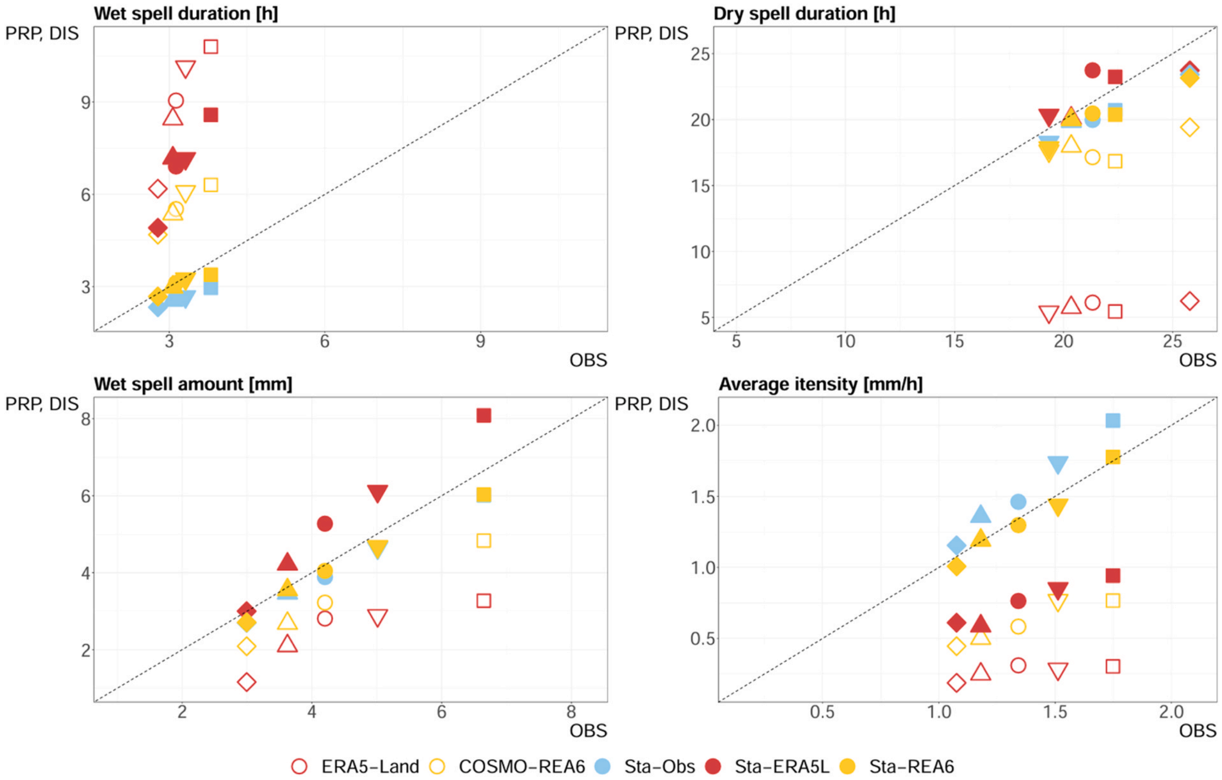

Fig. 3. Precipitation characteristics from disaggregated time series using different rainfall data for cascade model parameter estimation (Sta-Obs, Sta-ERA5L, Sta-REA6, all median values) and from PRP time series (ERA5-Land, COSMO-REA6) in comparison to observations (OBS) for each rain gauge as x-y-plot.

Table 2
MAE and PBIAS values for deviations of station-based and areal-based precipitation characteristics from PRP time series (ERA5-Land, COSMO-REA6) and disaggregated time series (Sta-Obs, Sta-ERA5L, Sta-REA6) using different rainfall data for cascade model parameter estimation.

Precipitation characteristic	Stations										Catchments									
	MAE					PBIAS [%]					MAE					PBIAS [%]				
	ERA5-Land	COSMO-REA6	Sta-Obs	Sta-ERA5L	Sta-REA6	ERA5-Land	COSMO-REA6	Sta-Obs	Sta-ERA5L	Sta-REA6	ERA5-Land	COSMO-REA6	Cat-Obs	Cat-ERA5L	Cat-REA6	ERA5-Land	COSMO-REA6	Cat-Obs	Cat-ERA5L	Cat-REA6
Wet spell duration (h)	5.7	2.4	0.4	3.7	0.1	175	74	−18	115	−4	5.4	3.2	−2.0	2.3	0.0	120	71	−42	52	2
Wet spell amount (mm)	−2.0	−1.0	0.2	0.8	0.3	−45	−22	−8	17	−6	−1.2	−0.8	−0.4	0.7	0.1	−29	−18	−8	20	6
Dry spell duration (h)	−16.0	−4.0	1.1	1.3	1.4	−73	−18	−6	2	−6	−11.8	−5.2	−2.4	−0.7	−1.7	−59	−23	−6	3	−3
Fraction of dry intervals (%)	−51.7	−18.5	0.0	0.1	0.0	−55	−20	2	−12	0	−37.8	−16.2	6.1	−7.5	−1.4	−47	−20	8	−9	−1
Average intensity (mm/h)	−1.1	−0.7	0.2	0.6	0.0	−81	−55	13	−45	−2	−0.6	−0.5	0.5	−0.2	0.0	−67	−52	62	−20	4

this study.

If the PRP time series are used for the cascade model parameter estimation and hence for the disaggregation of the observed daily time series, all deviations for the PRP identified before are reduced (Fig. 3, Table 2). While Sta-ERA5L still shows an overestimation of wet spell duration (PBIAS 115 %) and underestimation of the average intensity (-45 %), the results for the dry spell duration show an almost perfect fit to observations (2 %). For Sta-REA6 the disaggregation results show smaller or similar deviations for average intensity (-2 %), wet spell amount (-6 %), wet and dry spell duration (-4 % and −6 %, respectively). The goodness of Sta-REA6 results is similar to the parameter estimation using observed time series for dry spell duration and wet spell amount. For wet spell duration and average even intensity Sta-Rea6 outperforms Sta-Obs slightly.

The extreme values of the observed time series, PRP time series and disaggregated time series are shown for D= 1 h and D= 6 h for station D (i.e., Murska Sobota station) in Fig. 4. Station D was chosen since it has the longest time series, but the results are comparable for all stations. Both PRP underestimate the observed extreme values ($PBIAS_{D=1h,\ T=2\ yrs}$: −65 % for ERA5-Land and −13 % for COSMO-REA6, Table 3). For ERA5-Land the underestimation decreases with increasing duration. For REA6 underestimations occur only for D= 1 h and return periods T_n> 4 yrs. For longer durations, extreme values are well represented for the short return periods, while for higher return periods high overestimations are identified (for D=6 h and D=12 h for return periods T_n>16 yrs; for D=24 h for return periods T_n>10 yrs). Again, if the PRP time series are used for the estimation of the cascade model parameter, the deviations are reduced for both, Sta-ERA5L and Sta-REA6 (Fig. 4, Table 3). The highest deviations can be identified for D= 1 h with a slight less underestimation for Sta-REA6 ($PBIAS_{2\ yrs}$=9 %) than Sta-ERA5-Land ($PBIAS_{2\ yrs}$=-12 %). However, the usage of PRP data for parameter estimation is outperformed by the parameter estimation using observed time series, especially for the high return periods.

4.2. Catchment-based PRP validation

In Fig. 5 and Table 2 the catchment-based precipitation characteristics are shown. As for the station-based validation, ERA5-Land and COSMO-REA6 show the worst representation of the reference data set ARSO-h with strong overestimation of wet spell duration and underestimation of wet spell amount, dry spell duration, fraction of dry intervals and average intensity.

For the disaggregation of areal rainfall time series, all 20 catchments were used. It was shown before that the applied cascade model is capable of disaggregating point and areal rainfall time series (Müller-Thomy and Sikorska-Senoner, 2019; Maloku et al., 2024). For the disaggregation of the aggregated daily time series of ARSO-h, a practical approach is chosen by using the time series of the closest rain gauge for cascade model parameter estimation (Cat-Obs). The disaggregation results depend on the estimated parameters, which are provided for all data sets in the supplementary material C. In general, for Cat-Obs over- and underestimations differ among volume classes. While for the lower volume class the probabilities for generating dry time steps is overestimated by a station-based parameter estimation, they are underestimated for the upper volume class (vice versa for the probabilities leading to only wet time steps. These parameter deviations lead to shorter wet spell durations (caused by more frequent dry steps breaking one rainfall event on the coarser scale into two or more rainfall events on a finer scale), and hence to higher rainfall intensities for the fewer wet time steps (since the rainfall amount on the coarse scale remains identical).

For Cat-ERA5L and Cat-REA6, probabilities leading to dry time steps are underestimated, and probabilities leading to only wet time steps are overestimated. However, this pattern is less clear in comparison to the station-based validation (4.1). COSMO-REA6 leads to smaller parameter deviations than ERA5-Land.Cat-ERA5L and Cat-REA6 lead to better results than the direct usage of both PRP data sets (Fig. 5, Table 2). Also, Cat-REA6 outperforms Cat-ERA5L for wet spell amount, wet spell duration and average intensity. For dry spell duration the results are less clear. Artificial short dry spells resulting from the random generation of dry spells by P(1/0) and P(0/1) in the last disaggregation step(s) lower the average dry spell duration, leading to a systematic underestimation over the whole range and thus hiding the impact of data set choice for parameter estimation. Cat-REA6 also outperforms Cat-Obs. Cat-ERA5L is outperformed by Cat-Obs (wet spell duration and wet spell amount), only for average intensity Cat-ERA5L leads to better results.

For the catchment-based validation more detailed results are provided for catchment 1 (Mislinja catchment, northern Slovenia,

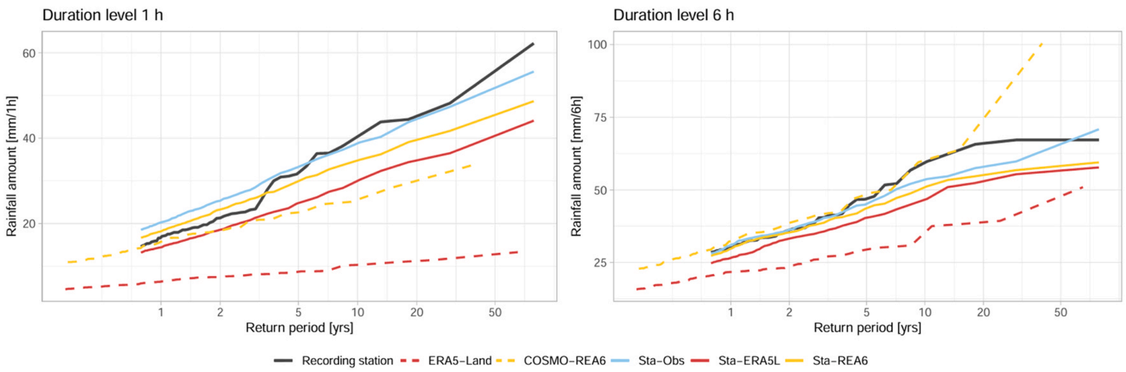

Fig. 4. Extreme values of station D (i.e., Murska Sobota) for D=1 h (left panel) and D=6 h (right panel) from observations, disaggregated time series using different rainfall data for cascade model parameter estimation (Sta-Obs, Sta-ERA5L, Sta-REA6) and from PRP time series (ERA5-Land, COSMO-REA6).

Table 3
PBIAS of extreme values for station D (i.e., Murska Sobota) and catchment 1 (i.e., Mislinja catchment) from disaggregated time series using different rainfall data for cascade model parameter estimation (Sta-Obs, Sta-ERA5L, Sta-REA6) and from PRP time series (ERA5-Land, COSMO-REA6).

Duration	Return period	Station D (Murska Sobota)					Catchment 1 (Mislinja catchment)				
		ERA5-Land	COSMO-REA6	Sta-Obs	Sta-ERA5L	Sta-REA6	ERA5-Land	COSMO-REA6	Cat-Obs	Cat-ERA5L	Cat-REA6
1 h	2 yrs	−65	−13	19	−13	9	−39	−21	30	−12	−1
	5 yrs	−72	−28	5	−22	−6	−31	−11	47	3	12
6 h	2 yrs	−34	7	0	−8	2	−41	−27	−2	−14	−8
	5 yrs	−37	5	−4	−14	−6	−41	−28	−3	−11	−8

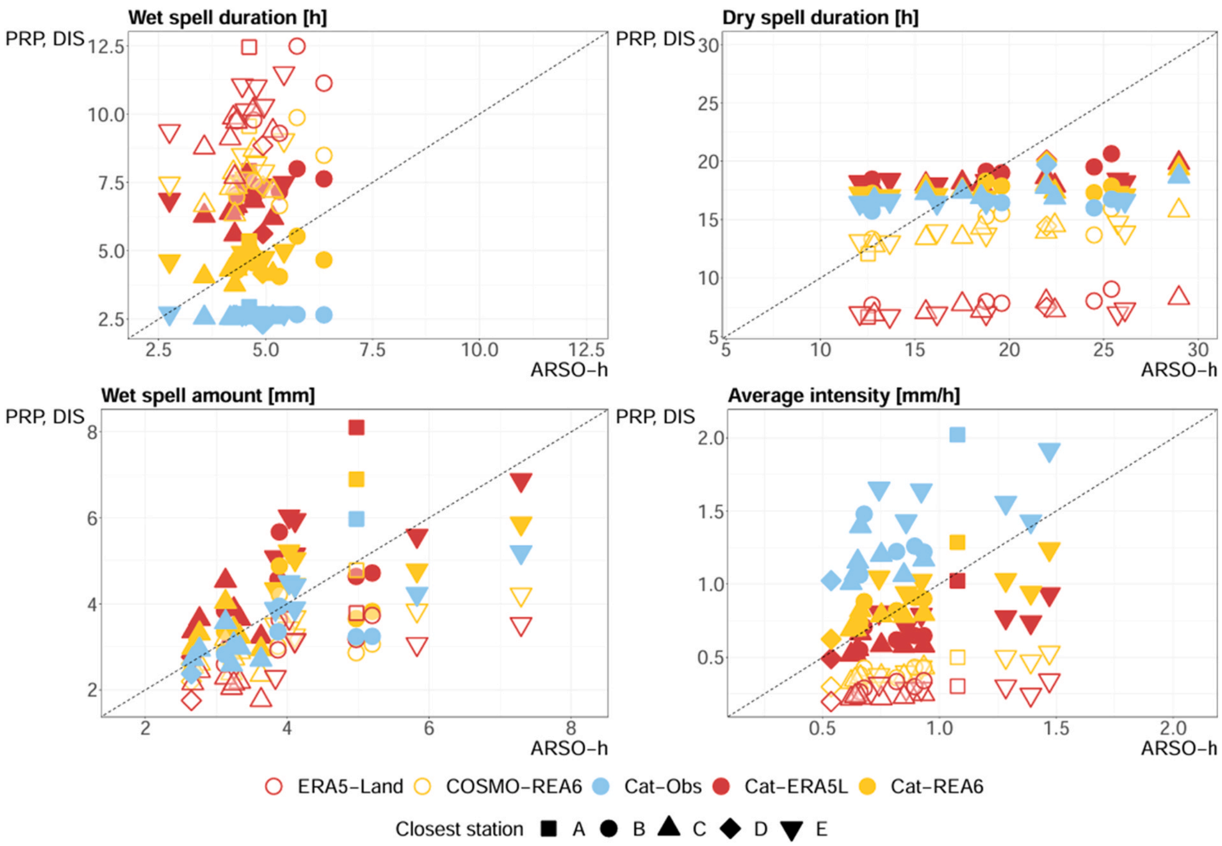

Fig. 5. Precipitation characteristics from disaggregated time series using different rainfall data for cascade model parameter estimation (Cat-Obs, Cat-ERA5L, Cat-REA6, all median values) and from PRP time series (ERA5-Land, COSMO-REA6) in comparison to ARSO-h as reference for each catchment as x-y-plot. The symbol indicates the closest rain gauge used for parameter estimation; the colour indicates the data sets.

closest rain gauge C within the catchment) and catchment 11 (Cerkniščica catchment, central Slovenia, non-mountainous region, closest rain gauge B outside of the catchment). The precipitation intensities of ARSO-h as reference data set and the disaggregated time series are shown as non-exceedance plots in Fig. 6 for catchment 11 (similar for all catchments). Only rainfall intensities ≥ 0.1 mm/h are considered since smaller intensities are less important from a hydrological point of view. Also, Molnar and Burlando (2005) and Müller and Haberlandt (2015), (2018) have shown that the cascade model tends to generate a high fraction of wet time steps with very small intensities. Hence, the considered rainfall intensities were restricted to avoid any distortion in the interpretation. As indicated in Table 4, the overestimation of P(x/(1-x)) by the PRPs leads to too many wet time steps in the disaggregated time series, which results in too small intensities.

While Cat-ERA5L underestimates ARSO-h as reference data set over the whole range, Cat-REA6 shows only underestimations for non-exceedance probabilities > 80 %. However, for < 70 % overestimations are identified for Cat-REA6. When the closest rain gauge is used for the parameter estimation, overestimations occur for the whole range of non-exceedance probabilities. Overall, CAT-REA6 shows the best representation of the non-exceedance curve of rainfall intensities for catchment 11.

In Fig. 7 the uncertainties for several precipitation characteristics are shown for catchment 11. The uncertainty from the 80 realizations of each disaggregation is for all presented precipitation characteristics neglectable in comparison to the uncertainty resulting

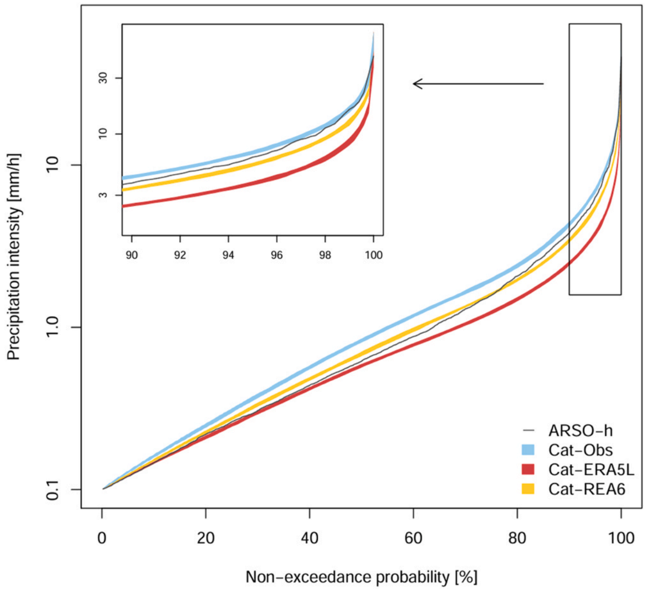

Fig. 6. Comparison of non-exceedance curves of rainfall intensities ≥ 0.1 mm for catchment 11 (i.e., Cerkniščica catchment). The line width results from the 80 realizations for each disaggregation.

Table 4
P-values from Spearman's rank correlation test (precipitation characteristic deviation vs. catchment attribute). Significant correlations (significance level 0.05 is used) are highlighted in green and bold, significances identified for both reanalysis products are underlined.

Precipitation characteristic	ERA5-Land			COSMO-REA6		
	Catchment size	Altitude maximum	Altitude mean	Catchment size	Altitude maximum	Altitude mean
Average intensity	**0.2 %**	6.8 %	**3.9 %**	**0.6 %**	18.4 %	11.5 %
Wet spell duration	21.0 %	**0.0 %**	**0.0 %**	73.8 %	**0.0 %**	**0.0 %**
Wet spell amount	**2.3 %**	78.2 %	95.5 %	14.1 %	**4.8 %**	9.0 %
Dry spell duration	**3.1 %**	10.7 %	15.4 %	**1.4 %**	15.0 %	20.2 %

from the choice of the data set used for parameter estimation. The results for Cat-REA6 enclose the ARSO-h values as reference data set for wet spell duration, wet spell amount and average intensity. Cat-ERA5-Land leads to better results than Cat-REA6 for only dry spell duration. The station-based parameters lead to the worst results for all precipitation characteristics analyzed (Cat-Obs).

In Fig. 8 the extreme values for catchment 1 are shown. The time series length of ARSO-h (5 years, 2006–2010) as reference data set limits the comparison of statistical representative return periods to $T_n \sim 2$ years. Higher return periods are only available with the disaggregation of the daily ARSO data set (available 1981–2010). As for the continuous precipitation characteristics, the extreme values directly derived from ERA5-Land and COSMO-REA6 lead to the strongest underestimations over the whole range of return periods (e.g. for D=6 h: $PBIAS_{2\ yrs}$=41 % for ERA5-Land and 27 % for COSMO-REA6, see Table 3). For both, Cat-ERA5L and Cat-REA6, the extreme values are well represented for $T_n < 5$ years, with slightly higher values for Cat-REA6. Cat-Obs leads to an overestimation of the extreme values for $T_n < 5$ years. The differences among the disaggregation-based approaches decrease with increasing extreme value durations.

4.3. Discussion and exploration of detected deviations

In general, ERA5-Land shows higher deviations from the reference data than COSMO-REA6 for both, gauge-based and catchment-based precipitation characteristics. A possible explanation is the coarser resolution in space of ERA5-Land (~81 km² raster size) in comparison to COSMO-REA6 (~36 km²), since reanalysis data with finer resolution can represent precipitation processes better (Gustafsson and Dahlgren, 2012; Wahl et al., 2017). This is especially important for regions with complex topography where precipitation characteristics can differ significantly over small scales (e.g., Bezak et al., 2021). For both PRP a Spearman's rank correlation test (Spearman, 1904, included in the R package 'Hmisc' by Harrell and Dupont, 2025) was applied. As a bivariate test, the correlation of precipitation characteristic deviations between ARSO-h as observations and ERA5-Land (or COSMO-REA6, respectively) as variable 1, and the catchment characteristics catchment size, maximum or mean altitude as variable 2 is determined. A *t*-test is used to test the significance of the correlation. If the resulting p-value is smaller than 0.05, the correlation is considered as significant (e.g., Breinl et al., 2021) with the consideration of the selected significance level (see Table 4). For average intensity and dry spell duration,

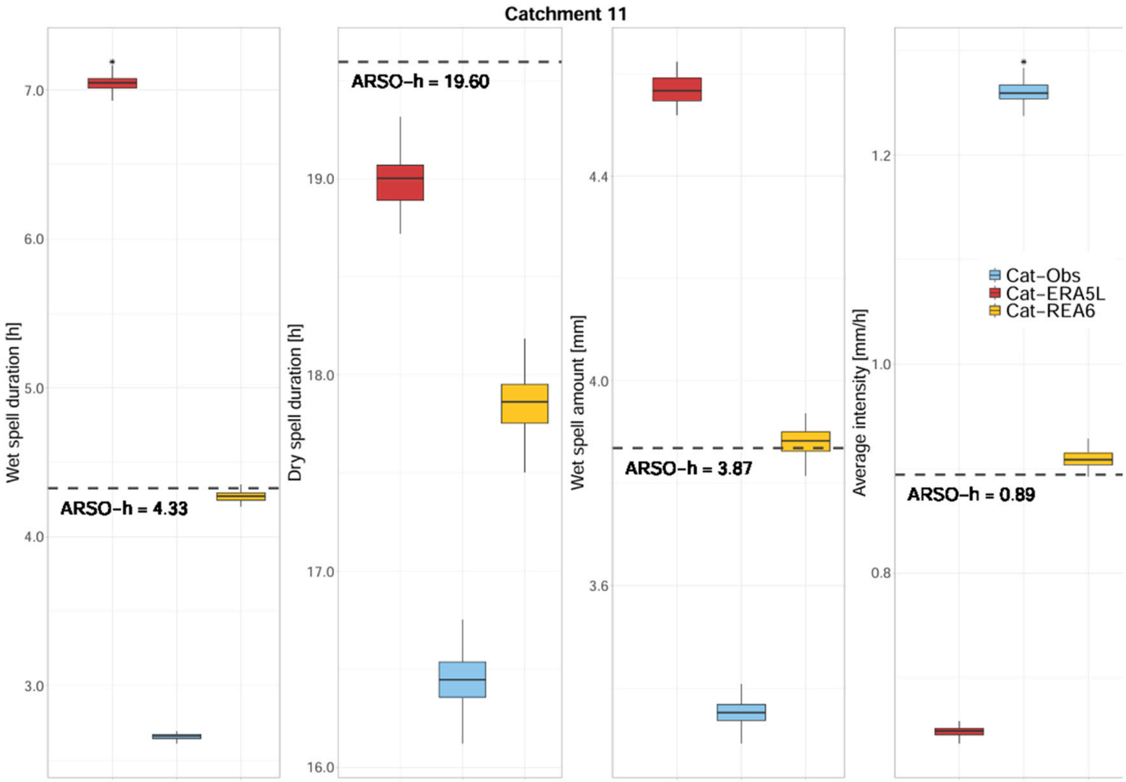

Fig. 7. Box-plots of precipitation characteristics for catchment 11 (I.e., Cerkniščica catchment).

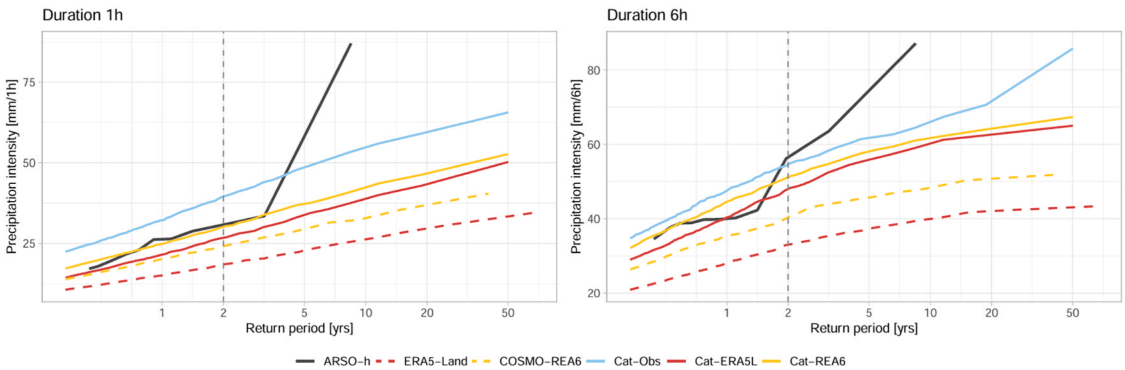

Fig. 8. Catchment-based extreme values for catchment 1 (i.e., Mislinja catchment) from observations, disaggregated time series using different rainfall data for cascade model parameter estimation (Cat-Obs, Cat-ERA5L, Cat-REA6) and from PRP time series (ERA5-Land, COSMO-REA6). The vertical dashed line indicates the limit for statistical representativity of ARSO-h as reference data set.

deviations for both PRP depend significantly on the catchment size. This is plausible, since both characteristics are highly affected by rainfall events with small spatial extent, which occur less frequently in smaller catchments. For wet spell duration, deviations for both PRP depend significantly on both, mean and maximum altitude of the catchment. While observed wet spell durations show no trend with increasing altitude, the deviations of both PRP show an increasing trend. Chen and Wen (2023) studied ERA5 data for China and identified an increasing number of false rainfall events with increasing altitude. With ERA5 as boundary condition this error transfers to ERA5-Land. Sharifi et al. (2019) also identified lower performance of ERA5 for high altitudes (elevation>1000 m) than in lower altitudes in terms of rainfall amounts for Austria. Sharifi et al. (2019) suspect the coarse spatial resolution of ERA5 to cause the identified deviations, which transfer to ERA5-Land.

5. Conclusions

In this study, the precipitation reanalysis products (PRP) ERA5-Land and COSMO-REA6 were validated for 5 rain gauges and 20 catchments in Slovenia. Furthermore, both PRP were tested as possible data sets to estimate the parameters of a micro-canonical cascade model to generate both, catchment- and gauge-based hourly precipitation time series from daily observations.

For the 5 rain gauges, both PRP lead to strong deviations from observed precipitation characteristics. Extreme values are underestimated for all return periods and all durations (for COSMO-REA6 only for D=1 h). These findings were expected due to the different spatial representation of precipitation behavior. The PRP were used for the cascade model parameter estimation and subsequent disaggregation of the daily precipitation amounts, which significantly improved the representation of observed precipitation characteristics.

The PRP were also compared with a merged product of observed radar and rain gauge data (ARSO-h) for 20 catchments (Cat-ERA5L and Cat-REA6). Both PRP show high deviations from observed areal precipitation characteristics with slightly better performance of COSMO-REA6.

The ARSO-h catchment precipitation time series were aggregated to daily values and then disaggregated to hourly values using cascade model parameters estimated from either Cat-ERA5L or Cat-REA6 PRP time series or from the closest observed rain gauge time series (Cat-Obs) for each catchment. The disaggregated catchment precipitation time series represent observed precipitation characteristics better than the PRP time series, including precipitation extreme values.

Similar to the rain gauge-based approach, the better representation of precipitation amounts on the daily scale by using ARSO observation data as input for the disaggregation, also the precipitation characteristics are represented better by the disaggregated time series than by the PRP directly. The disaggregation with parameters estimated from COSMO-REA6 outperforms both, ERA5-Land and rain gauge-based observations.

Significant dependencies of PRP precipitation characteristic deviations were identified for average intensity and dry spell duration (depending on catchment size) as well as wet spell duration (mean and maximum altitude). The results of this study indicate that rather than directly using the hourly PRP products it is advisable to estimate the parameters of the micro-canonical model based on the PRP data and disaggregate local daily datasets (with better spatial resolution) to hourly time series.

CRediT authorship contribution statement

Katarina Zabret: Writing – review & editing, Data curation. **Nejc Bezak:** Writing – review & editing, Supervision, Project administration, Funding acquisition, Data curation. **Patrick Nistahl:** Writing – review & editing, Supervision, Software, Formal analysis, Data curation. **Jana Kellner:** Writing – original draft, Visualization, Validation, Software, Investigation, Formal analysis, Data curation. **Kai Schröter:** Writing – review & editing, Supervision, Resources. **Hannes Müller-Thomy:** Writing – original draft, Validation, Supervision, Software, Project administration, Methodology, Funding acquisition, Formal analysis, Data curation, Conceptualization.

Open research

Code and data availability: Slovenian precipitation data from the Slovenian Environment Agency (ARSO) can be accessed via an online archive (https://meteo.arso.gov.si/met/sl/archive/), the radar data was provided on request. The COSMO-REA6 regional reanalysis is publicly available for direct download from the opendata-FTP server at DWD (https://opendata.dwd.de/climate_environment/REA/COSMO_REA6/, Source: Hans-Ertel-Centre for Weather Research) (DWD/HErZ, 2020). The Global ERA5-Land reanalysis is publicly available via the Copernicus Climate Data Store (CDS) (https://doi.org/10.24381/cds.e2161bac, Muñoz Sabater, 2019). The rainfall disaggregation program is written in Fortran and can be shared by the corresponding author on request.

Declaration of Competing Interest

The authors declare the following financial interests/personal relationships which may be considered as potential competing interests: Mueller-Thomy reports financial support was provided by German Academic Exchange Service. Nejc Bezak reports financial support was provided by Slovenian Research and Innovation Agency. Katarina Zabret reports financial support was provided by Slovenian Research and Innovation Agency. Jana Kellner reports financial support was provided by German Academic Exchange Service. Patrick Nistahl reports financial support was provided by German Academic Exchange Service. If there are other authors, they declare that they have no known competing financial interests or personal relationships that could have appeared to influence the work reported in this paper.

Acknowledgments

We would like to acknowledge the Slovenian Environment Agency (ARSO) for data provision. This research has been supported by the German Federal Ministry of Education and Research (BMBF) via Deutscher Akademischer Austauschdienst (grant no. 57569308). We declare that none of the authors has any competing interests. N.B and K.Z. contribution was supported by the Slovenian Research and Innovation Agency (ARIS) through grants P2-0180 and N2-0313.

Appendix A. Supporting information

Supplementary data associated with this article can be found in the online version at doi:10.1016/j.ejrh.2025.102530.

Data availability

Data access is indicated in the manuscript.

References

Acharya, S.C., Nathan, R., Wang, Q.J., Su, C.-H., 2022. Temporal disaggregation of daily rainfall measurements using regional reanalysis for hydrological applications. J. Hydrol. 610.

Alexopoulos, M.J., Müller-Thomy, H., Nistahl, P., Šraj, M., Bezak, N., 2023. Validation of precipitation reanalysis products for rainfall-runoff modelling in Slovenia. Hydrol. Earth Syst. Sci. 27, 2559–2578.

Bandhauer, M., Isotta, F., Lakatos, M., Lussana, C., Båserud, L., Izsák, B., Szentes, O., Tveito, O.E., Frei, C., 2022. Evaluation of daily precipitation analyses in E–OBS (v19.0e) and ERA5 by comparison to regional high–resolution data sets in european regions. Int. J. Climatol. 42 (2).

Berrisford, P., Dee, D.P., Fielding, K., Fuentes, M., Kållberg, P., Kobayashi, S., Uppala, S.M., 2009. The ERA-Interim archive. ERA Report Series, No. 1. ECMWF, Reading, UK.

Bezak, N., Petan, S., Mikos, M., 2021. Spatial and temporal variability in rainfall erosivity under alpine climate: a slovenian case study using optical disdrometer data. Front. Environ. Sci. 9, 735492. https://doi.org/10.3389/fenvs.2021.735492.

Bližňák, V., Pokorná, L., Rulfová, Z., 2022. Assessment of the capability of modern reanalyses to simulate precipitation in warm months using adjusted radar precipitation. J. Hydrol. Reg. Stud. 42, 101121.

Blöschl, G., Sivapalan, M., 1995. Scale issues in hydrological modelling: a review. Hydrol. Process. 9 (3-4), 251–290.

Bollmeyer, C., Keller, J.D., Ohlwein, C., Wahl, S., Crewell, S., Friederichs, P., Hense, A., Keune, J., Kneifel, S., Pscheidt, I., Redl, S., Steinke, S., 2015. Towards a high-resolution regional reanalysis for the european CORDEX domain. Q. J. R. Meteorol. Soc. 141, 1–15. https://doi.org/10.1002/qj.2486.

Breinl, K., Di Baldassarre, G., 2019. Space-time disaggregation of precipitation and temperature across different climates and spatial scales. J. Hydrol. Reg. Stud. 21, 126–146. https://doi.org/10.1016/j.ejrh.2018.12.002.

Breinl, K., Lun, D., Müller-Thomy, H., Blöschl, G., 2021. Understanding the relationship between rainfall and flood probabilities through combined intensity-duration-frequency analysis. J. Hydrol. 602, 126759.

Chen, H., Wen, D., 2023. Dependency of errors for four global reanalysis and satellite precipitation estiamtes on four crucial factors. Atmos. Res. 296, 107076. https://doi.org/10.1016/j.atmosres.2023.107076.

Dahlgren, P., Landelius, T., Kållberg, P., Gollvik, S., 2016. A high–resolution regional reanalysis for Europe. Part 1: three–dimensional reanalysis with the regional HIgh resolution Limited–Area model (HIRLAM). Q. J. R. Meteorol. Soc. 142 (698), 2119–2131.

Dalla Torre, D., Di Marco, N., Menapace, A., Avesani, D., Righetti, M., Majone, B., 2024. Suitability of ERA5-Land reanalysis dataset for hydrological modelling in the alpine region. J. Hydrol. Reg. Stud. 52, 101718.

Dee, D.P., Uppala, S.M., Simmons, A.J., Berrisford, P., Poli, P., Kobayashi, S., Andrae, U., Balmaseda, M.A., Balsamo, G., Bauer, P., Bechtold, P., Beljaars, A.C.M., van de Berg, L., Bidlot, J., Bormann, N., Delsol, C., Dragani, R., Fuentes, M., Geer, A.J., Haimberger, L., Healy, S.B., Hersbach, H., Hólm, E.V., Isaksen, L., Kållberg, P., Köhler, M., Matricardi, M., McNally, A.P., Monge-Sanz, B.M., Morcrette, J.-J., Park, B.-K., Peubey, C., de Rosnay, P., Tavolato, C., Thépaut, J.-N., Vitart, F., 2011. The ERA-Interim reanalysis: configuration and performance of the data assimilation system. Q. J. R. Meteorol. Soc. 137 (656), 553–597.

Derx, J., Müller-Thomy, H., Kilic, H.S., Cervero-Arago, S., Linke, R., Lindner, G., Walochnik, J., Sommer, R., Komma, J., Farnleitner, A.H., Blaschke, A.P., 2023. A probabilistic-deterministic approach for assessing climate change effects on infection risks downstream of sewage emissions from CSOs. Water Res. 247, 120746.

Ding, J., Wallner, M., Müller, H., Haberlandt, U., 2016. Estimation of instantaneous peak flow from maximum daily flow using the HBV hydrological model. Hydrol. Process. 30 (9), 1431–1448.

Dolšak, D., Bezak, N., Sraj, M., 2016. Temporal characteristics of rainfall events under three climate types in Slovenia (Part B). J. Hydrol. 541, 1395–1405. https://doi.org/10.1016/j.jhydrol.2016.08.047.

Dunkerley, D.L., 2019. Rainfall intensity bursts and the erosion of soils: an analysis highlighting the need for high temporal resolution rainfall data for research under current and future climates. Earth Surf. Dynam 7, 345–360. https://doi.org/10.5194/esurf-7-345 2019.

DWA-A 531: Starkregen in Abhängigkeit von Wiederkehrzeit und Dauer, Technical guideline of the DWA, Hennef, 2012.

DWD/HErZ: COSMO-REA6, Deutscher Wetterdienst (DWD) and Hans-Ertel Centre for Weather Research (HErZ, University of Bonn, Germany), ⟨http://reanalysis.meteo.uni-bonn.de/?COSMO-REA6⟩ (last access: 14 November 2024), 2020.

Ebers, N., Schröter, K., Müller-Thomy, H., 2024. Estimation of future rainfall extreme values by temperature-dependent disaggregation of climate model data. Nat. Hazards Earth Syst. Sci. 24, 2025–2043.

Evin, G., Favre, A.-C., Hingray, B., 2018. Stochastic generation of multi-site daily precipitation focusing on extreme events. Hydrol. Earth Syst. Sci. 22 (1), 655–672. https://doi.org/10.5194/hess-22-655-2018.

Gebremichael, G.G., Hossain, F., Erickson, T., Gao, H., Hopson, T., 2017. Evaluation of the performance of precipitation products for hydrological modeling over the upper blue Nile basin. J. Hydrol. 550, 406–418. https://doi.org/10.1016/j.jhydrol.2017.05.021.

Gu, L., Yin, J., Wang, S., Chen, J., Qin, H., Yan, X., He, S., Zhao, T., 2023. How well do the multi-satellite and atmospheric reanalysis products perform in hydrological modelling. J. Hydrol. 617, 128920. https://doi.org/10.1016/j.jhydrol.2022.128920.

Güntner, A., Olsson, J., Calver, A., Gannon, B., 2001. Cascade-based disaggregation of continuous rainfall time series: the influence of climate. Hydrol. Earth Syst. Sci. 5, 145–164. https://doi.org/10.5194/hess-5-145-2001.

Gustafsson, N., Dahlgren, P., 2012. Assimilating host model information into a limited area model. Tellus A Dyn. Meteorol. Oceanogr. 64 (1), 15836.

Harrell, F.E., Dupont, C.: Package 'Hmisc', URL: ⟨https://hbiostat.org/R/Hmisc/⟩, 16.03.2025.

Hersbach, H., Bell, B., Berrisford, P., Hirahara, S., Horányi, A., Muñoz-Sabater, J., Nicolas, J., Peubey, C., Radu, R., Schepers, D., Simmons, A., Soci, C., Abdalla, S., Abellan, X., Balsamo, G., Bechtold, P., Biavati, G., Bidlot, J., Bonavita, M., Chiara, G., De, Dahlgren, P., Dee, D., Diamantakis, M., Dragani, R., Flemming, J., Forbes, R., Fuentes, M., Geer, A., Haimberger, L., Healy, S., Hogan, R.J., Hólm, E., Janisková, M., Keeley, S., Laloyaux, P., Lopez, P., Lupu, C., Radnoti, G., Rosnay, P., de, Rozum, I., Vamborg, F., Villaume, S., Thépaut, J.-N., 2020. The ERA5 global reanalysis. Q. J. R. Meteorol. Soc. 146, 1999–2049. https://doi.org/10.1002/QJ.3803.

Isotta, F.A., Vogel, R., Frei, C., 2015. Evaluation of european regional reanalyses and downscalings for precipitation in the alpine region. Meteorol. Z. 24 (1), 15–37.

Jarvis, A., Reuter, H.I., Nelson, A., and Guevara, E.: Hole-filled seamless SRTM data V4, International Centre for Tropical Agriculture (CIAT), available at: ⟨http://srtm.csi.cgiar.org⟩, 2008.

Jones, D., Wang, W., Fawcett, R., 2009. High-quality spatial climate data-sets for Australia. Aust. Meteorol. Oceanogr. J. 58, 233–248. https://doi.org/10.22499/2.5804.003.

Kaiser-Weiss, A.K., Borsche, M., Niermann, D., Kaspar, F., Lussana, C., Isotta, F.A., van den Besselaar, E., van der Schrier, G., Undén, P., 2019. Added value of regional reanalyses for climatological applications. Environ. Res. Commun. 1 (7), 071004.

Kellner, J.: Niederschlagsdisaggregation mittels Reanalysedaten in Slowenien, Master thesis, Leichtweiß-Institute for Hydraulic Engineering and Water Resources, Dept. of Hydrology and River Basin Management, Faculty for Architecture, Civil Engineering and Environmental Sciences, TU Braunschweig (in German), 2022.

Krajewski, W.F., Lakshmi, V., Georgakakos, K.P., Jain, S.C., 1991. A Monte Carlo study of rainfall sampling effect on a distributed catchment model. Water Resour. Res. 27, 119–128.

Lockhoff, M., Zolina, O., Simmer, C., Schulz, J., 2019. Representation of precipitation characteristics and extremes in regional reanalyses and Satellite- and Gauge-Based estimates over Western and central Europe. J. Hydrometeorol. 20 (6), 1123–1145.

Maloku, K., Evin, G., Hingray, B., 2024. Generating hourly mean areal precipitation time series with an at-site weather generator in Switzerland. SERRA 38, 3737–3754.

Molnar, P., Burlando, P., 2005. Preservation of rainfall properties in stochastic disaggregation by a simple random cascade model. Atmos. Res. 77 (1–4), 137–151.

Müller, H.: Niederschlagsdisaggregation für hydrologische Modellierung, Proceedings of the Institute of Water Resources Management, Hydrology and Agricultural Hydraulic Engineering, Gottfried Wilhelm Leibniz Universität Hannover, 101, 182 pages (in German), ISSN 0343-8090, 2016.

Müller, H., Haberlandt, U., 2015. Temporal rainfall disaggregation with a cascade model: from single-station disaggregation to spatial rainfall. J. Hydrol. Eng. 20 (11), 04015026. https://doi.org/10.1061/(ASCE)HE.1943-5584.0001195.

Müller, H., Haberlandt, U., 2018. Temporal rainfall disaggregation using a multiplicative cascade model for spatial application in urban hydrology. J. Hydrol. 556, 847–864. https://doi.org/10.1016/j.jhydrol.2016.01.031.

Müller-Thomy, H., 2020. Temporal rainfall disaggregation: possibilities to improve the autocorrelation, 169-18 Hydrol. Earth Syst. Sci. 24. https://doi.org/10.5194/hess-24-169-2020.

Müller-Thomy, H., Sikorska-Senoner, A., 2019. Does the complexity in temporal precipitation disaggregation matter for a lumped hydrological model? Hydrol. Sci. J. 64 (12), 1453–1471. https://doi.org/10.1080/02626667.2019.1638926.

Müller-Thomy, H., Wallner, M., Förster, K., 2018. Rainfall disaggregation for hydrological modeling: is there a need for spatial consistence? Hydrol. Earth Syst. Sci. 22, 5259–5280.

Muñoz Sabater, J.: ERA5-Land hourly data from 1950 to present, Copernicus Climate Change Service (C3S) Climate Data Store (CDS) [data set], https://doi.org/10.24381/cds.e2161bac, 2019.

Muñoz-Sabater, J., Dutra, E., Agustí-Panareda, A., Albergel, C., Arduini, G., Balsamo, G., Boussetta, S., Choulga, M., Harrigan, S., Hersbach, H., Martens, B., Miralles, D.G., Piles, M., Rodríguez-Fernández, N.J., Zsoter, E., Buontempo, C., Thépaut, J.N., 2021. ERA5-Land: a state-of-the-art global reanalysis dataset for land applications, earth syst. Sci. Data 13, 4349–4383. https://doi.org/10.5194/essd-13-4349-2021.

Nicotina, L.E., Celegon, E., Alessi, Rinaldo, A., Marani, M., 2008. On the impact of rainfall patterns on the hydrologic response. W12401 Water Resour. Res. 44. https://doi.org/10.1029/2007WR006654.

Obled, C., Wendling, J., Beven, K., 1994. The sensitivity of hydro logical models to spatial rainfall patterns: an evaluation using observed data. J. Hydrol. 159, 305–333.

Ochoa-Rodriguez, S., Wang, L.P., Gires, A., Pina, R.D., Reinoso-Rondinel, R., Bruni, G., Ichiba, A., Gaitan, S., Cristiano, E., van Assel, J., Kroll, S., Murl`a-Tuyls, D., Tisserand, B., Schertzer, D., Tchiguirinskaia, I., Onof, C., Willems, P., ten Veldhuis, M.C., 2015. Impact of spatial and temporal resolution of rainfall inputs on urban hydrodynamic modelling outputs: a multi-catchment investigation. J. Hydrol. 531 (2), 389–407. https://doi.org/10.1016/j.jhydrol.2015.05.035.

Ogden, F.L., Julien, P.Y., 1993. Runoff sensitivity to temporal and spatial rainfall variability at runoff plane and small basin scales. Water Resour. Res. 29, 2589–2597.

Olsson, J., 1998. Evaluation of a scaling cascade model for temporal rainfall disaggregation. Hydrol. Earth Syst. Sci. 2 (1), 19–30.

Peel, M.C., Finlayson, B.L., McMahon, T.A., 2007. Updated world map of the Köppen-Geiger climate classification. Hydrol. Earth Syst. Sci. 11 (5), 1633–1644. https://doi.org/10.5194/hess-11-1633-2007.

Peleg, N., Fatichi, S., Paschalis, A., Molnar, P., Burlando, P., 2017. An advanced stochastic weather generator for simulat ing 2-D high-resolution climate variables. J. Adv. Model. Earth Syst. 9 (3), 1595–1627. https://doi.org/10.1002/2016ms000854.

Peleg, N., Molnar, P., Burlando, P., Fatichi, S., 2019. Exploring stochastic climate uncertainty in space and time using a gridded hourly weather generator. J. Hydrol. 571, 627–641. https://doi.org/10.1016/j.jhydrol.2019.02.010.

Peleg, N., Sinclair, S., Fatichi, S., Burlando, P., 2020. Downscaling climate projections over large and data sparse regions: methodological application in the Zambezi river basin. Int. J. Climatol. 40, 6242–6264.

Pidoto, R., Bezak, N., Müller-Thomy, H., Shehu, B., Callau-Beyer, A.C., Zabret, K., Haberlandt, U., 2022. Comparison of rainfall generators with regionalisation for the estimation of rainfall erosivity at ungauged sites. Earth Surf. Dynam 10, 851–863. https://doi.org/10.5194/esurf-10-851-2022.

Richardson, C.W., 1981. Stochastic simulation of daily precipitation, temperature, and solar radiation. Water Resour. Res. 17 (1), 182–190. https://doi.org/10.1029/WR017i001p00182.

Schilling, W., 1991. Rainfall data for urban hydrology: what do we need? Atmos. Res. 27 (1-3), 5–21.

Sevdari, K., Marmullaku, D., 2023. Technical university of Denmark, dataset. Shapefile Eur. Ctries. https://doi.org/10.11583/DTU.23686383.

Sharifi, E., Eitzinger, J., Dorigo, W., 2019. Performance of the State-Of-The-Art gridded precipitation products over mountainous terrain: a regional study over Austria. Remote Sens. 11. https://doi.org/10.3390/rs11172018.

Spearman, C., 1904. The proof and measurement of association between two things, 72-01 Am. J. Psychol. 15 (1). https://doi.org/10.2307/1412159.

Su, C.-H., Eizenberg, N., Steinle, P., Jakob, D., Fox-Hughes, P., White, C.J., Rennie, S., Franklin, C., Dharssi, I., Zhu, H., 2019. BARRA v1.0: the bureau of meteorology atmospheric high-resolution regional reanalysis for Australia. Geosci. Model Dev. 12, 2049–2068. https://doi.org/10.5194/gmd-12-2049-2019.

Wahl, S., Bollmeyer, C., Crewell, S., Figura, C., Friedrichs, P., Hense, A., Keller, J.D., Ohlwein, C., 2017. A novel convective-scale regional reanalysis COSMO-REA2: improving the representation of precipitation. Meteorol. Z. 26 (4), 345–361.

Wilks, D.S., 1998. Multisite generalization of a daily stochastic precipitation generation model. J. Hydrol. 210 (1-4), 178–191. https://doi.org/10.1016/S0022-1694(98)00186-3.

Xie, P., Joyce, R., Wu, S., Yoo, S.-H., Yarosh, Y., Sun, F., Lin, R., 2017. Reprocessed, bias-corrected CMORPH global high resolution precipitation estimates from 1998. J. Hydrometeorol. 18 (6), 1617–1641. https://doi.org/10.1175/jhm-d 16-0168.1.